Eigenfunctions and the integrated density of states on Archimedean tilings

Norbert Peyerimhoff and Matthias Täufer

Abstract. We study existence and absence of ℓ^2-eigenfunctions of the combinatorial Laplacian on the 11 Archimedean tilings of the Euclidean plane by regular convex polygons. We show that exactly two of these tilings (namely the $(3.6)^2$ "kagome" tiling and the (3.12^2) tiling) have ℓ^2-eigenfunctions. These eigenfunctions are infinitely degenerate and are constituted of explicitly described eigenfunctions which are supported on a finite number of vertices of the underlying graph (namely the hexagons and 12-gons in the tilings, respectively). Furthermore, we provide an explicit expression for the Integrated Density of States (IDS) of the Laplacian on Archimedean tilings in terms of eigenvalues of Floquet matrices and deduce integral formulas for the IDS of the Laplacian on the (4^4), (3^6), (6^3), $(3.6)^2$, and (3.12^2) tilings. Our method of proof can be applied to other $\mathbb{Z}^d$-periodic graphs as well.

1. Introduction and statement of results

The goal of this paper is to provide concrete formulas for the Integrated Density of States (IDS) on Archimedean tilings, viewed as combinatorial graphs, and to study existence or absence of ℓ^2-eigenfunctions for the associated Laplacians.

A *plane tiling by regular convex polygons* is a countable family of regular convex polygons covering the plane without gaps or overlaps. It is called *edge-to-edge* if the corners and sides of the polygons coincide with the vertices and edges of the tiling (see [8]). The *type* of a vertex of an edge-to-edge plane tiling by regular polygons describes the order of the polygons arranged cyclically around the vertex, for example the vertices in the honeycomb tiling are all of the type $(6.6.6) =: (6^3)$.

Definition 1.1. An *Archimedean tiling* is an edge-to-edge tiling of the plane by regular convex polygons such that all vertices are of the same type.

Archimedean tilings were systematically investigated in 1619 by Johannes Kepler in his book Harmonices Mundi [14] (see [5] for an English translation). Kepler found all 11 Archimedean tilings, namely with vertices of type (4^4), (3^6), (6^3), $(3.6)^2$, (3.12^2), (4.8^2), $(3^3.4^2)$, $(3^2.4.3.4)$, $(3.4.6.4)$, $(3^4.6)$, and $(4.6.12)$, cf. [8, pp. 59 and 63] and Figure 1 for an illustration.

(4^4) (3^6) (6^3)

$(3.6)^2$ (3.12^2) $(3^3.4^2)$ (4.8^2)

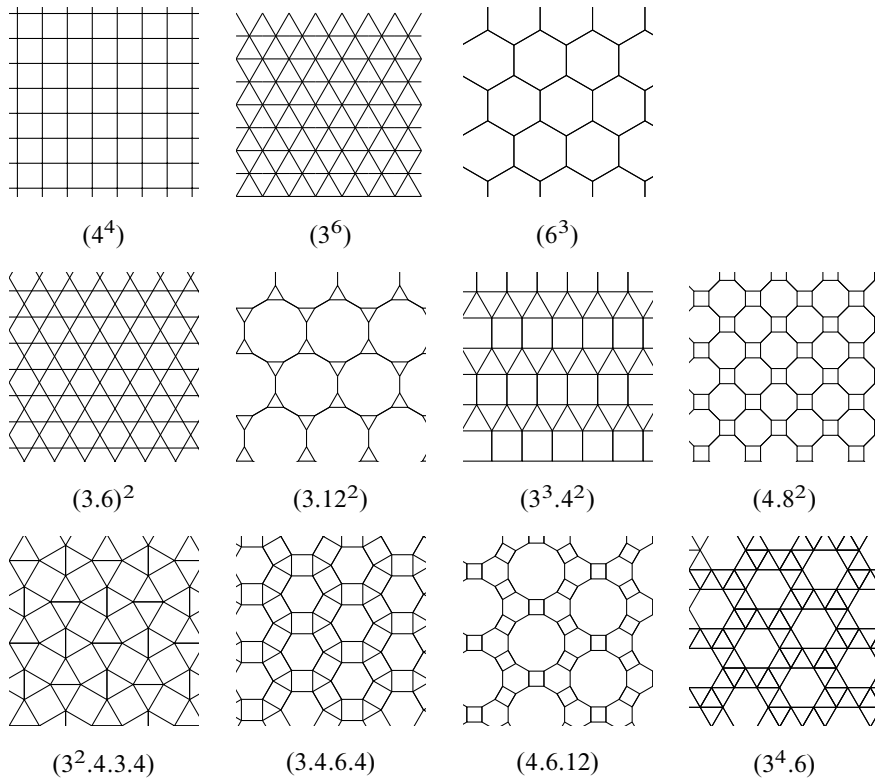$(3^2.4.3.4)$ $(3.4.6.4)$ $(4.6.12)$ $(3^4.6)$

Figure 1. The 11 Archimedean tilings.

There is a vast literature about various aspects of Archimedean tilings. For historical details on Archimedean tilings we refer the readers to [8, Section 2.10]. These tilings are relevant in crystallography as layers of stacked 3-dimensional structures [6, 7]. Archimedean tiling structures at different length scales have the potential to exhibit interesting properties: they may form frustrated magnets [9] or photonic crystals [31]. Diffusion constants of Archimedean tilings have been

calculated in [1]. Percolation thresholds of Archimedean solids have been investigated, e.g., in [30, 16, 29, 12, 27].

We view these tilings as combinatorial graphs $G = (\mathcal{V}, \mathcal{E})$ with vertex set $\mathcal{V}$ and edge set $\mathcal{E}$. The Laplacian $\Delta \colon \ell^2(\mathcal{V}) \to \ell^2(\mathcal{V})$ on such a graph is defined as

$$(\Delta f)(v) = f(v) - \frac{1}{|v|} \sum_{w \sim v} f(w), \tag{1}$$

where $|v|$ denotes the vertex degree of $v \in \mathcal{V}$, and $w \sim v$ means that w and v are adjacent, i.e. joined by an edge. This is a self-adjoint, bounded operator. On each of these graphs, there is a cofinite $\mathbb{Z}^2$-action allowing to define the Integrated Density of States (IDS) (for the precise definition see Section 2).

Our first main results are concrete integral expressions of the IDS for the Archimedean tilings (4^4), (3^6), (6^3), $(3.6)^2$, and (3.12^2). Moreover, we show that the tilings $(3.6)^2$ (kagome lattice), and (3.12^2) have Δ-eigenfunctions of finite support leading to jumps of the IDS. Finally, we show that no other Archimedean tiling has (any $\ell^2(\mathcal{V})$) eigenfunctions.

Remark 1.2. For periodic graphs with co-finite $\mathbb{Z}^d$ action, the (distributional) derivative of the IDS, the *density of states*, is a spectral measure in the sense that is carries all information on the spectrum: The points of increase of the IDS, i.e. the support of the density of states, are the spectrum of Δ [25, p. 119], see also [23, Proposition 5.2] for a proof of this statement in a more general context. The set of discontinuities of the IDS constitues the pure point spectrum and the singular continuous spectrum is empty [20, Theorem 6.10]. Thus, the remaining points of increase are the absolutely continuous spectrum. In particular, we have a complete description of the spectral types on all 11 Archimedean lattices.

Furthermore, since we have concrete expressions for the IDS of the tilings (4^4), (3^6), (6^3), $(3.6)^2$, and (3.12^2), it is straightforward to calculate their densities of states from our expressions below.

The method of proof is based on Floquet theory and can be applied to more general graphs with cofinite $\mathbb{Z}^d$-action and not only to Archimedean tilings. Examples include periodic finite hopping range operators on the nearest neighbour graph on $\mathbb{Z}^d$ or on non-planar, $\mathbb{Z}^2$-periodic graphs.

2. General results on the IDS and the lattice $\mathbb{Z}^d$

2.1. Floquet theory and the IDS. Even though the goal of this article will be to study the 11 (planar) graphs based on Archimedean tesselations, the results of this

subsection do not require planarity of the graph. More precisely, let $G = (\mathcal{V}, \mathcal{E})$ be an infinite graph with vertex set $\mathcal{V}$ and edge set $\mathcal{E}$. We assume that the vertex degree $|v|$ is finite for every $v \in \mathcal{V}$.

We also assume that there is a cofinite $\mathbb{Z}^d$-action on G, given by

$$\mathbb{Z}^d \ni \gamma \longmapsto T_\gamma \colon \mathcal{V} \longrightarrow \mathcal{V}.$$

Let $Q \subset \mathcal{V}$ be a (finite) fundamental domain of this action.

The graph Laplacian Δ, a self-adjoint bounded operator on $\ell^2(\mathcal{V})$, was defined in (1). The (abstract) Integrated Density of States (IDS) $N_G \colon \mathbb{R} \to [0, 1]$ of the Laplacian Δ on G is

$$N_G(E) := \frac{1}{|Q|} \operatorname{Tr}(\chi_Q \chi_{(-\infty, E]}(\Delta))$$

where $\chi_{(-\infty, E]}(\Delta)$ denotes the spectral projector onto the interval $(-\infty, E]$. Intuitively, the IDS counts the number of states of Δ below the energy level E per unit volume [22]. This is also reflected by formula (2) below. The IDS is non-decreasing and right continuous.

In order to apply Floquet theory, we also define the d-dimensional torus $\mathbb{T}^d = \mathbb{R}^d/(2\pi\mathbb{Z})^d$ and for every $\theta \in \mathbb{T}^d$ the $|Q|$-dimensional Hilbert space

$$\ell^2(\mathcal{V})_\theta := \{\tilde{f} \colon \mathcal{V} \longrightarrow \mathbb{C} \mid \tilde{f}(T_\gamma v) = e^{i\langle \theta, \gamma \rangle} \tilde{f}(v) \text{ for all } \gamma \in \mathbb{Z}^d\}$$

with inner product

$$\langle f, g \rangle_\theta := \sum_{v \in Q} f(v)\overline{g(v)}.$$

Furthermore, we define on $\ell^2(\mathcal{V})_\theta$ the θ-pseudoperiodic Laplacian Δ^θ as

$$\Delta^\theta f(v) := f(v) - \frac{1}{|v|} \sum_{w \sim v} f(w),$$

that is, Δ^θ acts in the same way as Δ but on the different vector space $\ell^2(\mathcal{V})_\theta$. Since this is a $|Q|$-dimensional vector space due to quasiperiodicity, the operator Δ^θ can be viewed as a hermitian $|Q| \times |Q|$-matrix. In Sections 3 and 4 we will give concrete examples of this matrix for the case of the 11 Archimedean lattice graphs. The map $\mathbb{T}^d \ni \theta \mapsto \sigma(\Delta^\theta)$ is also called *dispersion relation*.

The following theorem provides an integral expression for the IDS on $\mathbb{Z}^d$-periodic graphs, see also [20, Theorem 6.18].

Theorem 2.1. *We have*

$$N_G(E) = \frac{1}{(2\pi)^d |Q|} \int_{\mathbb{T}^d} \#\{\textit{Eigenvalues of } \Delta^\theta \textit{ less or equal than } E\} \, \mathrm{d}\theta. \quad (2)$$

For the convenience of the reader we now give a proof of Theorem 2.1 using Fourier theory on $\ell^2(\mathbb{Z}^d)$.

We have $\ell^2(\mathcal{V}) = \oplus_{v \in Q} \ell^2(\mathbb{Z}^d)$, where each summand $\ell^2(\mathbb{Z}^d)$ represents the space $\ell^2(\{T_\gamma v \mid \gamma \in \mathbb{Z}^d\})$. Therefore, we can isometrically identify $f \in \ell^2(\mathcal{V})$ with $(f_v)_{v \in Q} \in \oplus_{v \in Q} \ell^2(\mathbb{Z}^d)$ by $f_v(\gamma) := f(T_\gamma v)$. Applying the Fourier transform on every component, we obtain

$$\hat{f} \in \oplus_{v \in Q} L^2(\mathbb{T}^d), \quad \hat{f} := (\hat{f}_v)_{v \in Q}, \quad \text{where } \hat{f}_v(\theta) := \sum_{\gamma \in \mathbb{Z}^d} e^{-i\langle \theta, \gamma \rangle} f_v(\gamma).$$

From Fourier theory it follows that $f \mapsto \hat{f}$ is an isometry with the norms

$$\|f\|_{\ell^2(\mathcal{V})} := \sum_{v \in \mathcal{V}} |f(v)|^2 = \sum_{v \in Q} \sum_{\gamma \in \mathbb{Z}^d} |(T_\gamma v)|^2$$

and

$$\|\hat{f}\|_{\oplus_{v \in Q} L^2(\mathbb{T}^d)} := \sum_{v \in Q} \|\hat{f}_v\|_{L^2(\mathbb{T}^d)}^2 \quad \text{where } \|g\|_{L^2(\mathbb{T}^d)}^2 := \frac{1}{(2\pi)^d} \int_{\mathbb{T}^d} |g(\theta)|^2 \, d\theta.$$

We write $\tilde{f}_\theta(v) := \hat{f}_v(\theta)$ and extend $\tilde{f}_\theta(v)$ quasiperiodically to $\mathcal{V}$ via

$$\tilde{f}_\theta(T_\gamma v_0) = e^{i\langle \theta, \gamma \rangle} \tilde{f}_\theta(v_0), \quad \text{where } v_0 \in Q.$$

We have isometrically identified the spaces

$$\ell^2(\mathcal{V}) \simeq \int_{\mathbb{T}^d}^{\oplus} \ell^2(\mathcal{V})_\theta \, d\theta.$$

Lemma 2.2. *For all $v \in \mathcal{V}$, all $f \in \ell^2(\mathcal{V})$, and all $\theta \in \mathbb{T}^d$, we have*

$$\tilde{f}_\theta(v) = \sum_{\gamma \in \mathbb{Z}^d} e^{-i\langle \theta, \gamma \rangle} f(T_\gamma v). \tag{3}$$

Proof. Write $v = T_{\gamma_0} v_0$ for $v_0 \in Q$. Then

$$\begin{aligned}
\tilde{f}_\theta(v) &= \tilde{f}_\theta(T_{\gamma_0} v_0) = e^{i\langle \theta, \gamma_0 \rangle} \tilde{f}_\theta(v_0) \\
&= e^{i\langle \theta, \gamma_0 \rangle} \hat{f}_{v_0}(\theta) = \sum_{\gamma \in \mathbb{Z}^d} e^{i\langle \theta, \gamma_0 \rangle} e^{-i\langle \theta, \gamma \rangle} f(T_\gamma v_0) \\
&= \sum_{\gamma \in \mathbb{Z}^d} e^{-i\langle \theta, \gamma - \gamma_0 \rangle} f(T_{\gamma - \gamma_0} T_{\gamma_0} v_0) = \sum_{\gamma' \in \mathbb{Z}^d} e^{-i\langle \theta, \gamma' \rangle} f(T_{\gamma'} v). \qquad \square
\end{aligned}$$

Now, we can identify operators:

$$\Delta \cong \int\limits_{\theta \in \mathbb{T}^d}^{\oplus} \Delta^\theta \, \mathrm{d}\theta \quad \text{where} \, \Delta f(v) = f(v) - \frac{1}{|v|} \sum_{w \sim v} f(w) \qquad (4)$$

and where $\Delta f = g$, if and only if for all $v = T_{\gamma_0} v_0$ with $v_0 \in Q$,

$$\tilde{g}_\theta(v) \overset{(3)}{=} \sum_{\gamma \in \mathbb{Z}^d} e^{-i\langle \theta, \gamma \rangle} g(T_\gamma v)$$

$$= \sum_{\gamma \in \mathbb{Z}^d} e^{-i\langle \theta, \gamma \rangle} \Big[f(T_\gamma v) - \frac{1}{|T_\gamma v|} \sum_{w \sim T_\gamma v} f(w) \Big]$$

$$\overset{(3)}{=} \tilde{f}_\theta(v) - \frac{1}{|v|} \sum_{\gamma \in \mathbb{Z}^d} \sum_{w' \sim v} e^{-i\langle \theta, \gamma \rangle} f(T_\gamma w')$$

$$= \tilde{f}_\theta(v) - \frac{1}{|v|} \sum_{w \sim v} \sum_{\gamma \in \mathbb{Z}^d} e^{-i\langle \theta, \gamma \rangle} f(T_\gamma w)$$

$$\overset{(3)}{=} \tilde{f}_\theta(v) - \sum_{w \sim v} \frac{1}{|v|} \tilde{f}_\theta(w) = \Delta^\theta \tilde{f}_\theta(v).$$

Recall that Δ^θ and Δ are formally defined via the same expressions, but they operate on different spaces: Δ operates on ℓ^2-functions on G while Δ^θ operates on θ-quasiperiodic functions.

From (4), we conclude

$$\chi_{(-\infty, E]}(\Delta) \cong \int\limits_{\mathbb{T}^d}^{\oplus} \chi_{(-\infty, E]}(\Delta^\theta) \, \mathrm{d}\theta.$$

and therefore

$$\widetilde{(\chi_{(-\infty, E]}(\Delta) f)}_\theta = \chi_{(-\infty, E]}(\Delta^\theta) \tilde{f}_\theta$$

Now, we are in a position to calculate the IDS. We have

$$N_G(E) = \frac{1}{|Q|} \operatorname{Tr}(\chi_Q \chi_{(-\infty, E]}(\Delta)) = \frac{1}{|Q|} \sum_{v \in Q} \langle \delta_v, \chi_{(-\infty, E]}(\Delta) \delta_v \rangle$$

$$= \frac{1}{(2\pi)^d |Q|} \sum_{v \in Q} \int\limits_{\mathbb{T}^d} \langle (\widetilde{\delta_v})_\theta, \widetilde{(\chi_{(-\infty, E]}(\Delta^\theta) \delta_v)}_\theta \rangle \, \mathrm{d}\theta$$

$$= \frac{1}{(2\pi)^d |Q|} \int\limits_{\mathbb{T}^d} \sum_{v \in Q} \langle (\widetilde{\delta_v})_\theta, \chi_{(-\infty, E]}(\Delta^\theta) \widetilde{\delta_v})_\theta \rangle \, \mathrm{d}\theta.$$

The operator, $\chi_{(-\infty, E]}(\Delta^{\theta})$ is an orthogonal projection onto the finite-dimensional span of eigenfunctions of Δ^{θ} on $\ell^2(Q)$ with eigenvalues smaller or equal than E (i.e. a matrix). Hence, the trace $\text{Tr}(\chi_{(-\infty, E]}(\Delta^{\theta}))$ is the number of eigenvalues of Δ^{θ} less or equal than E. This finishes the proof of Theorem 2.1.   □

The next results are useful to show absence of finitely supported eigenfunctions for particular graphs.

Theorem 2.3. *The following are equivalent*:

(i) N_G *is continuous at* E;

(ii) Δ *has no eigenfunctions with eigenvalue* E *of finite support*;

(iii) Δ *has no* $\ell^2(\mathcal{V})$*-eigenfunctions with eigenvalue* E;

(iv) *There is* $\theta \in \mathbb{T}^d$ *such that* $E \notin \sigma(\Delta^{\theta})$.

Corollary 2.4. *If there exist* $\theta, \theta' \in \mathbb{T}^d$ *such that* $\sigma(\Delta^{\theta}) \cap \sigma(\Delta^{\theta'}) = \emptyset$, *then* N_G *is continuous.*

Proof of Theorem 2.3. The equivalence of items (i), (ii) and (iii) is proved in [19], see also [24, Corollary 2.3] for a proof in a more general setting.

It remains to show the equivalence of (i) and (iv). We fix $E \in \mathbb{R}$ and calculate, using the dominated convergence theorem,

$$N_G(E) - \lim_{E' \nearrow E} N_G(E')$$

$$= \frac{1}{(2\pi)^d |Q|} \int_{\mathbb{T}^d} \lim_{E' \nearrow E} \#\{\text{Eigenvalues of } \Delta^{\theta} \text{ in } (E', E]\} \, \mathrm{d}\theta$$

$$= \frac{1}{(2\pi)^d |Q|} \int_{\mathbb{T}^d} \{\text{Multiplicity of the eigenvalue } E \text{ of } \Delta^{\theta}\} \, \mathrm{d}\theta.$$

This is non-zero if and only if the characteristic polynomial

$$P_{\Delta^{\theta}}(E) := \det(\Delta^{\theta} - E \cdot \text{Id})$$

vanishes on a set $S \subset \mathbb{T}^d$ of positive measure. Since $\theta \mapsto P_{\Delta^{\theta}}(E)$ is a real analytic function, this is equivalent to $P_{\Delta^{\theta}}(E)$ vanishing identically on $\mathbb{T}^d$ (see [18, p. 67]). Thus discontinuity of N_G at E is equivalent to $E \in \sigma(\Delta^{\theta})$ for all $\theta \in \mathbb{T}^d$.   □

Let us note that the analytic nature of the band functions has been used in similar arguments before, see e.g. [20, Corollary 6.19].

2.2. The lattice $\mathbb{Z}^d$. As a first application of (2), we calculate the IDS of Δ on the lattice $\mathbb{Z}^d$. An elementary cell Q consists of a single point. In the 2-dimensional case, we can view $\mathbb{Z}^2$ as a tiling by unit squares (i.e. as the (4^4) tiling) with $\mathbb{Z}^2$ generated by translation vectors $\omega_1 = (1, 0)$, and $\omega_2 = (0, 1)$, cf. Figure 2. The (1×1)-matrix corresponding to Δ^θ has the entry (and hence the only eigenvalue)

$$\lambda_{\mathbb{Z}^d}^\theta = 1 - \frac{1}{2d}(e^{-i\theta_1} + e^{i\theta_1} + \cdots + e^{-i\theta_d} + e^{i\theta_d}) = 1 - \frac{1}{d}\sum_{j=1}^d \cos(\theta_j). \quad (5)$$

Thus, (2) simplifies to

$$N_{\mathbb{Z}^d}(E) = \frac{1}{(2\pi)^d} \operatorname{Vol}\left\{\theta \in \mathbb{T}^d : \frac{1}{d}\sum_{j=1}^d \cos(\theta_j) \geq 1 - E\right\}. \quad (6)$$

It is clear that $N_{\mathbb{Z}^d}(E)$ is supported in $[0, 2]$. Moreover, by Corollary 2.4, the IDS on $\mathbb{Z}^d$ is continuous and Δ has no ℓ^2-eigenfunctions since from (5) we conclude $\lambda_{\mathbb{Z}^d}^\theta = 0 \neq 2 = \lambda_{\mathbb{Z}^d}^{\theta'}$ for $\theta = (0, \ldots, 0)$, and $\theta' = (\pi, \ldots, \pi)$.

In dimensions $d = 1, 2$, the following expressions for the IDS follow directly from (6). In the case $d = 2$, we derive the expression by applying the substitution $t = \cos\theta_1$.

Proposition 2.5. *In dimension $d = 1$, we have*

$$N_{\mathbb{Z}}(E) = \frac{\chi_{[0,2]}(E)}{\pi} \cdot \arccos(1 - E).$$

In dimension $d = 2$, we have

$$\begin{aligned}
N_{\mathbb{Z}^2}(E) &= N_{(4^4)}(E) \\
&= \frac{1}{(2\pi)^2} \operatorname{Vol}\{\theta \in \mathbb{T}^2 \mid \cos\theta_1 + \cos\theta_2 \geq 2 - 2E\} \\
&= \begin{cases}
0 & \text{if } E < 0, \\
\dfrac{1}{\pi^2} \displaystyle\int_{1-2E}^1 \frac{\arccos(2 - 2E - t)}{\sqrt{1 - t^2}}\, dt & \text{if } 0 \leq E \leq 1, \\
1 - N_{(4^4)}(2 - E) & \text{if } 1 < E \leq 2, \\
1 & \text{if } 2 < E.
\end{cases}
\end{aligned}$$

$(a + \omega_2)$

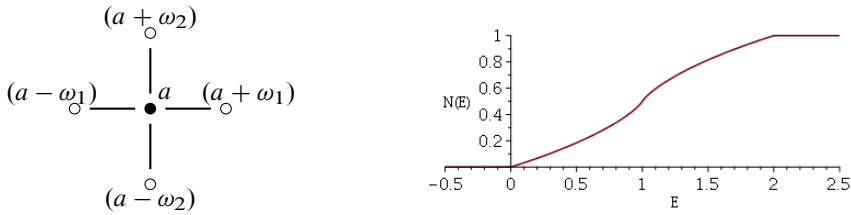$(a - \omega_1)$ a $(a + \omega_1)$

$(a - \omega_2)$

Figure 2. Fundamental domain of the graph $\mathbb{Z}^2$ (left) and its IDS (right).

3. Concrete integral expressions for the IDS of some Archimedean tilings

In this section, we present concrete integral expressions of the IDS of the Archimedean tilings with vertex types (3^6), (6^3), $(3.6)^2$, and (3.12^2). We will denote the corresponding IDS by $N_{(3^6)}$, etc.

We will see that only the last two tilings admit finitely supported eigenfunctions.

3.1. IDS of the (3^6) tiling (triangular lattice). A fundamental domain consists of a single point with translation vectors $\omega_1 = (1, 0)$, $\omega_2 = (\cos(\pi/3), \sin(\pi/3))$, cf. Figure 3. The corresponding matrix Δ^θ has the only entry and hence the only eigenvalue

$$\lambda^\theta_{(3^6)} = \left(1 - \frac{1}{6}(e^{i\theta_1} + e^{-i\theta_1} + e^{i\theta_2} + e^{-i\theta_2} + e^{i(\theta_2 - \theta_1)} + e^{-i(\theta_2 - \theta_1)})\right)$$

$$= \left(1 - \frac{1}{3}(\cos(\theta_1) + \cos(\theta_2) + \cos(\theta_2 - \theta_1))\right).$$

Therefore,

$$N_{(3^6)}(E) = \frac{1}{(2\pi)^2} \operatorname{Vol}\left\{\theta \in \mathbb{T}^2 : \frac{1}{3}(\cos(\theta_1) + \cos(\theta_2) + \cos(\theta_2 - \theta_1)) \geq 1 - E\right\}.$$

$$(7)$$

$(a - \omega_1 + \omega_2)$ $(a + \omega_2)$

$(a - \omega_1)$ a $(a + \omega_1)$

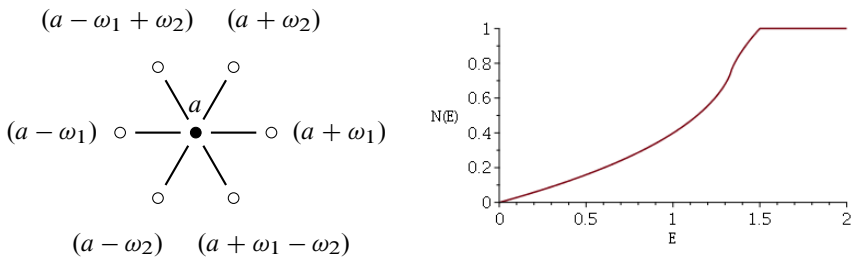$(a - \omega_2)$ $(a + \omega_1 - \omega_2)$

Figure 3. Fundamental domain of the (3^6) tiling (left) and its IDS (right).

Since the expression

$$\mathrm{Vol}\{\theta \in \mathbb{T}^2 : \cos(\theta_1) + \cos(\theta_2)) + \cos(\theta_2 - \theta_1) \geq L\}$$

will be relevant later on, we shall discuss it in more detail here. By periodicity, we can consider $\mathbb{T}^2$ as $(-\pi, \pi)^2$ (the boundary is a measure zero set and does not play any role). Using the change of variables $u := (\theta_1 + \theta_2)/\sqrt{2}$, $v = (\theta_1 - \theta_2)/\sqrt{2}$ we find

$$\cos(\theta_1) + \cos(\theta_2) + \cos(\theta_1 - \theta_2) = \cos\left(\frac{u+v}{\sqrt{2}}\right) + \cos\left(\frac{u-v}{\sqrt{2}}\right) + \cos\left(\sqrt{2}u\right)$$

$$= 2\cos\left(\frac{u}{\sqrt{2}}\right)\cos\left(\frac{v}{\sqrt{2}}\right) + 2\cos^2\left(\frac{u}{\sqrt{2}}\right) - 1.$$

The new variables (u, v) identify $\mathbb{T}^2$ with the domain

$$\Diamond := \{(u, v) \in \mathbb{R}^2 : |u| + |v| < \pi\sqrt{2}\}.$$

Lemma 3.1. *The function* $F : \Diamond \to \mathbb{R}$, *defined by*

$$F(u, v) = 2\cos\left(\frac{u}{\sqrt{2}}\right)\cos\left(\frac{v}{\sqrt{2}}\right) + 2\cos^2\left(\frac{u}{\sqrt{2}}\right) - 1$$

has the following properties:

  i) *the global maximum of* F *is at* $(u, v) = (0, 0)$, *where* $F(u, v) = 3$;

 ii) *the two global minima of* F *are at* $(u, v) = (\pm 2/3 \cdot \sqrt{2}\pi, 0)$, *where* $F(u, v) = -3/2$;

iii) $F \geq -1$ *in the "hexagon"* (Hex) $:= \{(u, v) \in \Diamond : |u| \leq \pi/\sqrt{2}\}$ *and* $F \leq -1$ *in the complemetary set* (Tri)$_-$ $\cup$ (Tri)$_+$ *which consists of two rectangular triangles*;

 iv) *we have*

$$\mathrm{Vol}\{F \geq L\} = \begin{cases} (2\pi)^2 & \text{if } L < -3/2, \\[2ex] (2\pi^2) - 8\displaystyle\int_{-1/2-\frac{1}{2}\sqrt{2L+3}}^{-1/2+\frac{1}{2}\sqrt{2L+3}} \frac{\arccos\left(\frac{L+1}{2t} - t\right)}{\sqrt{1-t^2}}\,\mathrm{d}t & \text{if } -3/2 \leq L < -1, \\[3ex] 8\displaystyle\int_{-\frac{1}{2}+\frac{1}{2}\sqrt{2L+3}}^{1} \frac{\arccos\left(\frac{L+1}{2t} - t\right)}{\sqrt{1-t^2}}\,\mathrm{d}t & \text{if } -1 \leq L < 3, \\[3ex] 0 & \text{if } 3 \leq L. \end{cases}$$

Remark 3.2. It is known that additional symmetries (e.g. a rotational symmetry) of the underlying graph are reflected in symmetries of the dispersion relation. More precisely, in an appropriate basis, the function F is symmetric under rotations by $\pi/3$ around its maximum and symmetric under rotations by $2\pi/3$ around its minima. This corresponds to symmetries of the underlying graph, see [2, Lemma 2.1] for details.

Proof. It is straightforward to check i) to iii) and using symmetry and monotonicity considerations

$$
\text{Vol}\{F \geq L\}
$$
$$
= \begin{cases}
(2\pi)^2 & \text{if } L < -3/2, \\
(2\pi)^2 - 2 \cdot \text{Vol}\{(u,v) \in (\text{Tri})_+ : F(u,v) \geq L\} & \text{if } -3/2 \leq L < -1, \\
4 \cdot \text{Vol}\{(u,v) \in (\text{Hex}) \cap \mathbb{R}_+^2 : F(u,v) \geq L\} & \text{if } -1 \leq L < 3, \\
0 & \text{if } 3 \leq L.
\end{cases}
$$
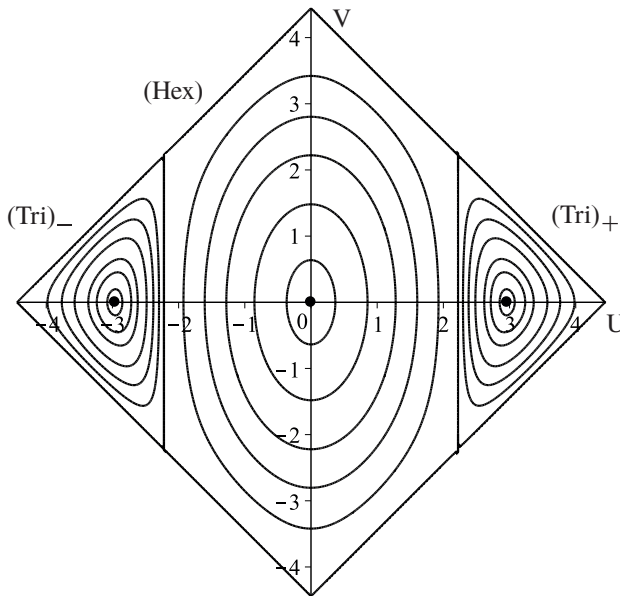
Figure 4. Level sets of the function $F: \diamond \to \mathbb{R}$ and the domains (Hex) and $(\text{Tri})_\pm$.

To calculate the area within $(\text{Tri})_+$ we consider the upper half (i.e. $v \geq 0$) of $(\text{Tri})_+$ (i.e. $u \geq \pi/\sqrt{2}$). Therein, $\cos(u/\sqrt{2}) < 0$, whence $F(u, v) \leq L$ is equivalent to

$$\cos\left(\frac{v}{\sqrt{2}}\right) \geq \frac{L+1}{2\cos\left(\frac{u}{\sqrt{2}}\right)} - \cos\left(\frac{u}{\sqrt{2}}\right). \tag{8}$$

and we found that the area is the area under a graph. Since $\cos(v/\sqrt{2}) \leq 1$, we conclude that (8) can only be fulfilled if u is in the interval between the two solutions of $\cos(u/\sqrt{2}) = (L+1)/2 - \cos^2(u/\sqrt{2})$ in $(\pi/\sqrt{2}, \sqrt{2}\pi)$, i.e. for

$$u \in (u_-, u_+) := \left(\sqrt{2}\arccos\left(-1/2 + \frac{1}{2}\sqrt{2L+3}\right),\right.$$
$$\left.\sqrt{2}\arccos\left(-1/2 - \frac{1}{2}\sqrt{2L+3}\right)\right).$$

Together with (8), we find

$$\text{Vol}\{(u, v) \in (\text{Tri})_+ \colon F(u, v) \geq L\}$$
$$= 2\int_{u_-}^{u_+} \sqrt{2}\arccos\left(\frac{L+1}{2\cos\left(\frac{u}{\sqrt{2}}\right)} - \cos\left(\frac{u}{\sqrt{2}}\right)\right) du$$
$$= \int_{-1/2-\frac{1}{2}\sqrt{2L+3}}^{-1/2+\frac{1}{2}\sqrt{2L+3}} 4\frac{\arccos\left(\frac{L+1}{2t} - t\right)}{\sqrt{1-t^2}} dt$$

where in the last step, we used the transformation $u = \sqrt{2}\arccos(t)$.

As for the area in the hexagon H, by an analogous argument,

$$\text{Vol}\{(u, v) \in (\text{Hex}) \cap \mathbb{R}_+^2 \colon F(u, v) \geq L\}$$
$$= \int_0^{u_0} \sqrt{2}\arccos\left(\frac{L+1}{2\cos(u/\sqrt{2})} - \cos(u/\sqrt{2})\right) du$$
$$= 2\int_{-\frac{1}{2}+\frac{1}{2}\sqrt{2L+3}}^{1} \frac{\arccos\left(\frac{L+1}{2t} - t\right)}{\sqrt{1-t^2}} dt$$

where

$$u_0 = \sqrt{2}\arccos\left(-\frac{1}{2} + \frac{1}{2}\sqrt{2L+3}\right)$$

is the solution of $\cos(u/\sqrt{2}) = (L+1)/2 - \cos^2(u/\sqrt{2})$ in $[0, \pi/\sqrt{2}]$. $\qquad\square$

Combining Lemma 3.1 and (7), we find:

Proposition 3.3. *We have*

$$N_{(3^6)}(E) = \frac{1}{(2\pi)^2} \operatorname{Vol}\{(u, v) \in \diamond \colon F(u, v) \geq 3 - 3E\}$$

$$= \begin{cases} 0 & \text{if } E < 0, \\[2mm] \dfrac{2}{\pi^2} \displaystyle\int\limits_{-\frac{1}{2}+\frac{1}{2}\sqrt{9-6E}}^{1} \dfrac{\arccos\left(\frac{4-3E}{2t} - t\right)}{\sqrt{1-t^2}}\,dt & \text{if } 0 \leq E < \dfrac{4}{3}, \\[6mm] 1 - \dfrac{2}{\pi^2} \displaystyle\int\limits_{-1/2-\frac{1}{2}\sqrt{9-6E}}^{-1/2+\frac{1}{2}\sqrt{9-6E}} \dfrac{\arccos\left(\frac{4-3E}{2t} - t\right)}{\sqrt{1-t^2}}\,dt & \text{if } \dfrac{4}{3} \leq E < \dfrac{3}{2}, \\[6mm] 1 & \text{if } 3/2 < E. \end{cases}$$

In particular, $N_{(3^6)}$ is continuous and there are no ℓ^2-eigenfunctions.

3.2. IDS of the (6^3) (honeycomb) tiling. The honeycomb tiling is of particular practical interest since this structure appears in graphene and is closely related to fullerenes (buckeyballs) and carbon nano-tubes. The earliest reference from which the dispersion relations for this tiling can be inferred seems to be [32]. Furthermore, parts of our calculations have an overlap with the metric graph investigations in [21], where the authors derive dispersion relations and determine various spectral types of the Hamiltonian not only for the (6^3) tiling, but also for metric nano-tube graphs isometrically embedded in cylinders. Moreover, [4] is a good source to find further information and references about graphene under a magnetic field.

A fundamental domain is $Q = \{a, b\} = \{(0, 0), (0, 1)\}$, cf. Figure 5. This implies

$$\Delta^\theta = \begin{pmatrix} 1 & -\frac{1}{3}(1 + e^{i\theta_1} + e^{i\theta_2}) \\ -\frac{1}{3}(1 + e^{-i\theta_1} + e^{-i\theta_2}) & 1 \end{pmatrix}$$

which has the eigenvalues

$$\begin{cases} \lambda_{(6^3),1}^\theta = 1 - \dfrac{1}{3}\sqrt{2\cos\theta_1 + 2\cos\theta_2 + 2\cos(\theta_1 - \theta_2) + 3}, \\[3mm] \lambda_{(6^3),2}^\theta = 1 + \dfrac{1}{3}\sqrt{2\cos\theta_1 + 2\cos\theta_2 + 2\cos(\theta_1 - \theta_2) + 3}. \end{cases}$$
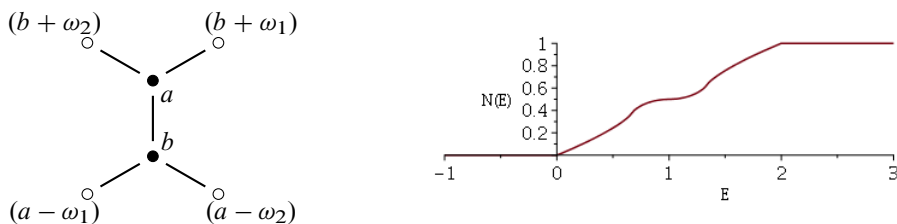
Figure 5. Fundamental domain of the (6^3) tiling (left) and its IDS (right).

Therefore,

$$N_{(6^3)}(E) = \frac{1}{2(2\pi)^2}(\mathrm{Vol}\{\theta \in \mathbb{T}^2 : \lambda^\theta_{(6^3),1} \le E\} + \mathrm{Vol}\{\theta \in \mathbb{T}^2 : \lambda^\theta_{(6^3),2} \le E, \}).$$

We see that $N_{(6^3)}(E)$ has support $[0, 2]$ and is antisymmetric around $(E, N(E)) = (1, 1/2)$. For $E < 1$, we find by Lemma 3.1

$$N_{(6^3)}(E) = \frac{1}{2(2\pi)^2} \mathrm{Vol}\{\theta \in \mathbb{T}^2 : \lambda^\theta_{(6^3),1} \le E\}$$

$$= \frac{1}{2(2\pi)^2} \mathrm{Vol}\left\{(u, v) \in \diamond : F(u, v) \ge \frac{9}{2}(1 - E)^2 - 3/2\right\}.$$

Therefore, using Lemma 3.1 and antisymmetry around $E = 1$, we find the following result.

Proposition 3.4. *We have*

$$N_{(6^3)}(E) = \begin{cases} 0 & \text{if } E < 0 \\[2mm] \dfrac{1}{\pi^2} \displaystyle\int\limits_{1-\frac{3}{2}E}^{1} \dfrac{\arccos\left(\frac{9(1-E)^2-1}{4t} - t\right)}{\sqrt{1-t^2}}\, \mathrm{d}t & \text{if } 0 \le E < 2/3 \\[4mm] \dfrac{1}{2} - \dfrac{1}{\pi^2} \displaystyle\int\limits_{-2+\frac{3}{2}E}^{1-\frac{3}{2}E} \dfrac{\arccos\left(\frac{9(1-E)^2-1}{4t} - t\right)}{\sqrt{1-t^2}}\, \mathrm{d}t & \text{if } 2/3 \le E < 1 \\[4mm] \dfrac{1}{2} + \dfrac{1}{\pi^2} \displaystyle\int\limits_{1-\frac{3}{2}E}^{-2+\frac{3}{2}E} \dfrac{\arccos\left(\frac{9(E-1)^2-1}{4t} - t\right)}{\sqrt{1-t^2}}\, \mathrm{d}t & \text{if } 1 \le E < 4/3 \\[4mm] 1 - \dfrac{1}{\pi^2} \displaystyle\int\limits_{1-\frac{3}{2}E}^{1} \dfrac{\arccos\left(\frac{9(E-1)^2-1}{4t} - t\right)}{\sqrt{1-t^2}}\, \mathrm{d}t & \text{if } 4/3 \le E < 2 \\[4mm] 1 & \text{if } 2 \le E. \end{cases}$$

In particular, there are no ℓ^2-eigenfunctions.

3.3. IDS of the $(3.6)^2$ tiling ("the kagome lattice").

Properties of kagome lattice structures under magnetic fields have been investigated both in the Applied Physics literature (e.g., [33] and references therein studying kagome staircase compounds) and in the Theoretical Physics literature (butterfly-type spectra for ultracold atoms in optical kagome lattices, see [11, 15, 10] and references therein, as well as [3]). We refer the readers also to [26] for historical information on the name "kagome" and how the scientific community became interested in this structure.
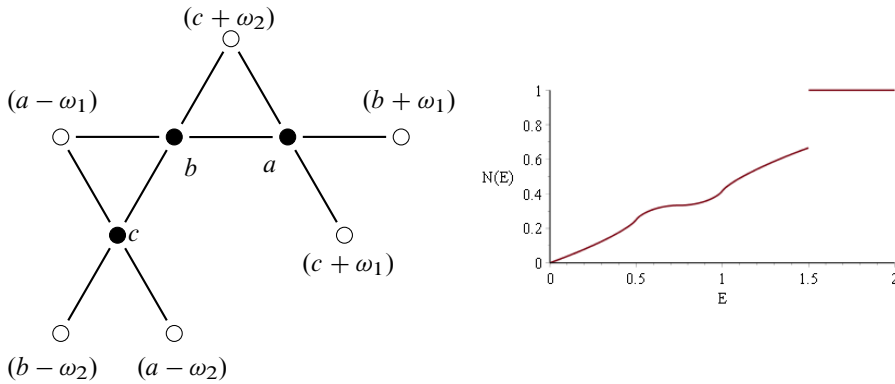
Figure 6. Fundamental domain of the $(3.6)^2$ tiling (left) and its IDS (right).

We would like to point out that jumps and strict monotonicity properties of the IDS of the combinatorial Laplacian on the kagome lattice were already determined in [22, Proposition 3.3]. We now derive an explicit formula for the IDS.

A fundamental domain of the kagome lattice consists of three points, cf. Figure 6. This leads to the matrix

$$\Delta^\theta = \mathrm{Id} - \frac{1}{4}\begin{pmatrix} 0 & (1+e^{i\theta_1}) & (e^{i\theta_1}+e^{i\theta_2}) \\ (1+e^{-i\theta_1}) & 0 & (1+e^{i\theta_2}) \\ (e^{-i\theta_1}+e^{-i\theta_2}) & (1+e^{-i\theta_2}) & 0 \end{pmatrix}$$

with eigenvalues

$$\begin{cases} \lambda^\theta_{(3.6)^2,1} = \dfrac{3-\sqrt{3+2F(u,v)}}{4}, \\ \lambda^\theta_{(3.6)^2,2} = \dfrac{3+\sqrt{3+2F(u,v)}}{4}, \\ \lambda^\theta_{(3.6)^2,3} = \dfrac{3}{2}. \end{cases}$$

Furthermore the eigenvalue $3/2$ of Δ^θ is θ-independent whence by Theorem 2.3, it corresponds to an infinitely degenerate eigenvalue of Δ. It can be seen that this eigenvalue is a linear combination of finitely supported eigenvalues on each

hexagon where at the vertices of the hexagon, the eigenfunction takes the values ± 1 in alternating order, see also Figure 8. From Lemma 3.1, we deduce the following result.

Proposition 3.5. *We have*

$$N_{(3.6)^2}(E) = \frac{1}{3(2\pi)^2} \sum_{k=1}^{3} \mathrm{Vol}\{\theta \in \mathbb{T}^2 : \lambda_{(3.6)^2,k}^{\theta} \le E\}$$

$$= \begin{cases} 0 & \text{if } E < 0 \\[2mm] \dfrac{2}{3\pi^2} \displaystyle\int\limits_{1-2E}^{1} \dfrac{\arccos\left(\frac{4E^2-6E+2}{t} - t\right)}{\sqrt{1-t^2}}\,\mathrm{d}t & \text{if } 0 \le E < \dfrac{1}{2} \\[5mm] \dfrac{1}{3} - \dfrac{2}{3\pi^2} \displaystyle\int\limits_{2E-2}^{1-2E} \dfrac{\arccos\left(\frac{4E^2-6E+2}{t} - t\right)}{\sqrt{1-t^2}}\,\mathrm{d}t & \text{if } \dfrac{1}{2} \le E < \dfrac{3}{4} \\[5mm] \dfrac{1}{3} + \dfrac{2}{3\pi^2} \displaystyle\int\limits_{1-2E}^{2E-2} \dfrac{\arccos\left(\frac{4E^2-6E+2}{t} - t\right)}{\sqrt{1-t^2}}\,\mathrm{d}t & \text{if } \dfrac{3}{4} \le E < 1 \\[5mm] \dfrac{2}{3} - \dfrac{2}{3\pi^2} \displaystyle\int\limits_{2E-2}^{1} \dfrac{\arccos\left(\frac{4E^2-6E+2}{t} - t\right)}{\sqrt{1-t^2}}\,\mathrm{d}t & \text{if } 1 \le E < \dfrac{3}{2} \\[5mm] 1 & \text{if } \dfrac{3}{2} < E. \end{cases}$$

For each hexagon H there exists (up to scalar multiples) exactly one eigenfunction with support on H. Every ℓ^2-eigenfunction is a linear combination of these special finitely supported eigenfunctions.

3.4. IDS of the (3.12^2) tiling. The (3.12^2) tiling is the second Archimedean tiling after the $(3.6)^2$ (kagome) tiling which has compactly supported eigenfunctions. It also has the interesting feature that the spectrum consists of the two intervals $[0, 2/3]$ and $[1, 5/3]$, i.e. it has a proper band structure which might make nanomaterials based on this tiling an interesting candidate for applications.

A fundamental domain consists of six points, $Q = \{a, b, c, d, e, f\}$, cf. Figure 7. We have

$$\Delta^{\theta} = \mathrm{Id} - \frac{1}{3}\begin{pmatrix} 0 & 1 & 1 & 0 & e^{-i\theta_2} & 0 \\ 1 & 0 & 1 & 0 & 0 & e^{i\theta_1} \\ 1 & 1 & 0 & 1 & 0 & 0 \\ 0 & 0 & 1 & 0 & 1 & 1 \\ e^{i\theta_2} & 0 & 0 & 1 & 0 & 1 \\ 0 & e^{-i\theta_1} & 0 & 1 & 1 & 0 \end{pmatrix}.$$

Its characteristic polynomial is

$$P_{\Delta^\theta}(E) = \frac{(E-1)(3E-5)}{243}(81E^4 - 270E^3 + 279E^2 - 90E$$
$$- 2(\cos(\theta_1) + \cos(\theta_2) + \cos(\theta_1 - \theta_2) - 3))$$
$$= \frac{(E-1)(3E-5)}{243}(81E^4 - 270E^3 + 279E^2 - 90E - 2F(u,v) + 6),$$

where we used again the change of variables $u := (\theta_1 + \theta_2)/\sqrt{2}$, $v = (\theta_1 - \theta_2)/\sqrt{2}$ and the function F from Lemma 3.1. This is a polynomial of degree 6 and its roots are

$$\lambda^\theta_{(3.12^2,1)} = \frac{1}{6}(5 - \sqrt{13 + 4\sqrt{2F(u,v)+3}}) \in \left[0, \frac{5-\sqrt{13}}{6}\right],$$

$$\lambda^\theta_{(3.12^2,2)} = \frac{1}{6}(5 - \sqrt{13 - 4\sqrt{F(u,v)+3}}) \in \left[\frac{5-\sqrt{13}}{6}, \frac{2}{3}\right],$$

$$\lambda^\theta_{(3.12^2,3)} = 1,$$

$$\lambda^\theta_{(3.12^2,4)} = \frac{1}{6}(5 + \sqrt{13 - 4\sqrt{F(u,v)+3}}) \in \left[1, \frac{5+\sqrt{13}}{6}\right],$$

$$\lambda^\theta_{(3.12^2,5)} = \frac{1}{6}(5 + \sqrt{13 + 4\sqrt{2F(u,v)+3}}) \in \left[\frac{5+\sqrt{13}}{6}, \frac{5}{3}\right],$$

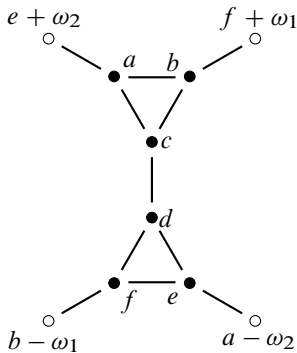$$\lambda^\theta_{(3.12^2,6)} = \frac{5}{3}.$$
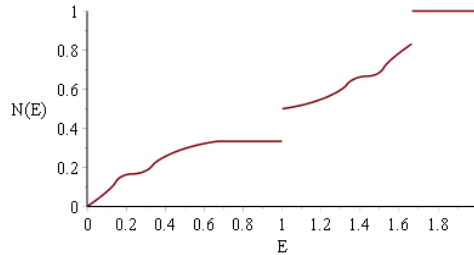
Figure 7. Fundamental domain of the (3.12^2) tiling (left) and its IDS (right).

We see that the spectrum of Δ is supported in the two bands $[0, 2/3]$ and $[1, 5/3]$. Furthermore the eigenvalues 1 and $5/3$ of Δ^θ are θ-independent whence by Theorem 2.3, they correspond to two linearly independent, infinitely degenerate supported eigenvalues of Δ. It can be seen that the corresponding space of eigenfunctions is spanned by functions which are supported on the vertices of a single 12-gon where cyclically at the vertices of the 12-gon either the values $1, -1, 1, -1, \ldots$ (in case $\lambda = 5/3$) or the values $1, 1, -1, -1, 1, 1, \ldots$ (in case $\lambda = 1$) appear, see also Figure 8.
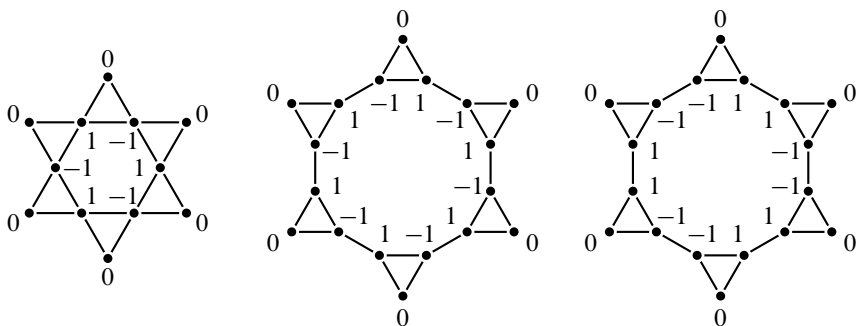
Figure 8. Eigenfunction in the $(3.6)^2$ tesselation with support on a single hexagon (left) and the two types of eigenfunctions in the (3.12^2) tesselation with support on a single 12-gon (center and right).

Using some elementary algebra and Theorem 2.1, we find the following result.

Proposition 3.6. *We have*

$$N_{(3.12^2)}(E) = \frac{1}{6(2\pi)^2} \sum_{k=1}^{6} \text{Vol}\left\{\theta \in \mathbb{T}^2 : \lambda_{(3.12^2, k)} \leq E\right\}.$$

Introducing

$$I(a, b) = \frac{1}{3\pi^2} \int_a^b \arccos\left(\frac{-\frac{1}{2} + \frac{9}{2}(3E^2 - 5E + 1)^2}{2t} - t\right) \frac{dt}{\sqrt{1 - t^2}}$$

and

$$A_- = -\frac{1}{2} - \frac{3}{2}(3E^2 - 5E + 1), \quad A_+ = -\frac{1}{2} + \frac{3}{2}(3E^2 - 5E + 1),$$

this leads to:

- *if $E < 0$,*
$$N_{(3.12^2)}(E) = 0;$$

- *if $0 \leq E < \frac{5-\sqrt{17}}{6}$,*
$$N_{(3.12^2)}(E) = I\left(A_+, 1\right);$$

- *if $\frac{5-\sqrt{17}}{6} \leq E < \frac{5-\sqrt{13}}{6}$,*
$$N_{(3.12^2)}(E) = \frac{1}{6} - I\left(A_-, A_+\right);$$

- *if $\frac{5-\sqrt{13}}{6} \leq E < \frac{1}{3}$,*
$$N_{(3.12^2)}(E) = \frac{1}{6} + I\left(A_-, A_+\right);$$

- *if $\frac{1}{3} \leq E < \frac{2}{3}$,*
$$N_{(3.12^2)}(E) = \frac{1}{3} - I\left(A_+, 1\right);$$

- *if $\frac{2}{3} \leq E < 1$,*
$$N_{(3.12^2)}(E) = \frac{1}{3};$$

- *if $1 \leq E < \frac{4}{3}$,*
$$N_{(3.12^2)}(E) = \frac{1}{2} + I(A_+, 1),$$

- *if $\frac{4}{3} \leq E < \frac{5+\sqrt{13}}{6}$,*
$$N_{(3.12^2)}(E) = \frac{2}{3} - I(A_-, A_+),$$

- *if $\frac{5+\sqrt{13}}{6} \leq E < \frac{5+\sqrt{17}}{6}$,*
$$N_{(3.12^2)}(E) = \frac{2}{3} + I(A_-, A_+),$$

- *if $\frac{5+\sqrt{17}}{6} \leq E < \frac{5}{3}$,*
$$N_{(3.12^2)}(E) = \frac{5}{6} - I(A_+, 1),$$

- *if $\frac{5}{3} \leq E$,*
$$N_{(3.12^2)}(E) = 1.$$

For each 12-*gon D there exist* (*up to scalar multiples*) *exactly two linearly in-dependent eigenfunctions with support on D. Every ℓ^2-eigenfunction is a linear combination of one type of these special finitely supported eigenfunctions.*

We refer to Figure 7 for a plot of $N_{(3.12^2)}$.

Remark 3.7. The eigenfunctions on the $(6.3)^2$ and the (3.12^2) are (finite or infinite) linear combinations of eigenfunctions supported on a single hexagon or 12-gon, respectively, see Figure 8 for an illustration. One observes that both these tesselations share the feature that they contain an $2n$-gon which is either completely surrounded by triangles or where triangles are adjacent to every second edge. Since the $(3.6)^2$ tiling and the (3.12^2) tiling are the only ones with this property, this might give an intuitive explaination why exactly these two tilings have finitely supported eigenfunctions. However, if one considers periodic graphs which are not based on a tesselation by regular polygons the situation might be different. Figure 9 gives an example of a (non-archimedean) tesselation with finitely supported eigenfunctions.
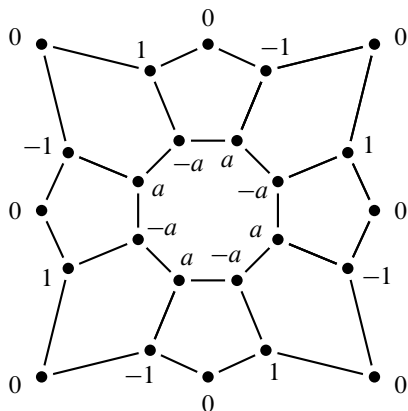

Figure 9. An example of an elementary cell of a planar, periodic, but non-Archimedean tiling with finitely supported eigenfunctions where the choice $a = 1 \pm \sqrt{2}$ yields an eigenfunctions to the eigenvalue $\lambda = 1 + a/3$.

4. Absence of ℓ^2-eigenfunctions on the remaining Archimedean tilings

We show in this section that the remaining Archimedean tilings, namely $(3^3.4^2)$, (4.8^2), $(3^2.4.3.4)$, $(3.4.6.4)$, $(4.6.12)$, and $(3^4.6)$ do not have ℓ^2-eigenfunctions.

Therefore, their IDS' are continuous whence – in the light of the discussion in Remark 1.2 – their have purely absolutely continuous spectrum. Sufficient geometric conditions for the absence of finitely supported eigenfunctions in plane tessellations, based on combinatorial curvature, were given in [17, 13] (see also [28] about the topic of finitely supported eigenfunctions and unique continuation). These curvature conditions are not satisfied in the examples under consideration, so we need to employ Theorem 2.3 instead. Since we do not always have explicit expressions of the eigenvalues of the operators Δ^θ or the volumes of their sublevels sets are too difficult to handle, we will not provide explicit integral expressions for these IDS', but we are still able to exclude the existence of ℓ^2-eigenfunctions. In fact, for each tiling, we will find the θ-dependent matrix Δ^θ, make two choices $\theta, \theta' \in \mathbb{T}^2$, and see that the sets of eigenvalues of Δ^θ and $\Delta^{\theta'}$ are disjoint.

4.1. IDS of the $(3^3.4^2)$ tiling. A fundamental domain consists of two points $\{a, b\}$ as in Figure 10. This leads to the matrix

$$\Delta^\theta = \mathrm{Id} - \frac{1}{5} \begin{pmatrix} e^{i\theta_1} + e^{-i\theta_1} & 1 + e^{i\theta_2} + e^{i(\theta_2 - \theta_1)} \\ 1 + e^{-i\theta_2} + e^{-i(\theta_2 - \theta_1)} & e^{i\theta_1} + e^{-i\theta_1} \end{pmatrix}.$$

with eigenvalues

$$\lambda_\pm = 1 - \frac{2}{5} \cos(\theta_1) \pm \frac{1}{5} |1 + e^{i(\theta_1 - \theta_2)} + e^{i\theta_2}|$$

$$= 1 - \frac{2}{5} \cos(\theta_1) \pm \frac{1}{5} \sqrt{3 + 2\cos(\theta_1) + 2\cos(\theta_2) + 2\cos(\theta_2 - \theta_1)}.$$
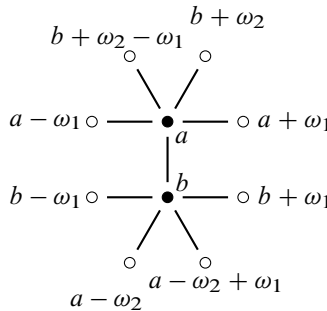

Figure 10. Fundamental domain of the $(3^3.4^2)$ tiling.

Plugging in $\theta = (0, 0)$ and $\theta = (0, \pi)$, we find

$$\sigma(\Delta^{(0,0)}) = \left\{0, \frac{6}{5}\right\} \quad \text{and} \quad \sigma(\Delta^{(0,\pi)}) = \left\{\frac{2}{5}, \frac{4}{5}\right\}.$$

Since these sets are disjoint, Theorem 2.3 and Corollary 2.4 imply

Proposition 4.1. *The* $(3^3.4^2)$ *tiling has no* $\ell^2(\mathcal{V})$-*eigenfunctions.*

4.2. IDS of the (4.8^2) tiling. A fundamental domain consists of the four vertices $\{a, b, c, d\}$ adjacent to a square, cf. Figure 11.
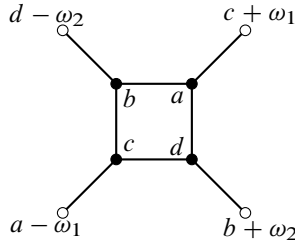

Figure 11. Fundamental domain of the (4.8^2) tiling.

It leads to the matrix

$$\Delta^\theta = \text{Id} - \frac{1}{3}\begin{pmatrix} 0 & 1 & e^{i\theta_1} & 1 \\ 1 & 0 & 1 & e^{-i\theta_2} \\ e^{-i\theta_1} & 1 & 0 & 1 \\ 1 & e^{i\theta_2} & 1 & 0 \end{pmatrix}$$

Inserting the values $\theta = (0,0)$ and $\theta = (\pi, \pi)$, we find

$$\sigma(\Delta^{(0,0)}) = \left\{0, \frac{4}{3}\right\} \quad \text{and} \quad \sigma(\Delta^{(\pi,\pi)}) = \left\{\frac{2}{3}, 2\right\}.$$

Since the spectra are disjoint, Theorem 2.3 and Corollary 2.4 imply the following result.

Proposition 4.2. *The* (4.8^2) *tiling has no* $\ell^2(\mathcal{V})$-*eigenfunctions.*

4.3. IDS of the $(3^2.4.3.4)$ tiling. A fundamental domain consists of the four vertices $\{a, b, c, d\}$ adjacent to a square with edges parallel to the axes, cf. Figure 12. It leads to the matrix

$$\Delta^\theta = \text{Id} - \frac{1}{5}\begin{pmatrix} 0 & 1 + e^{i\theta_2} & e^{i\theta_1} & 1 + e^{i\theta_1} \\ 1 + e^{-i\theta_2} & 0 & 1 + e^{i\theta_1} & e^{-i\theta_2} \\ e^{-i\theta_1} & 1 + e^{-i\theta_1} & 0 & 1 + e^{-i\theta_2} \\ 1 + e^{-i\theta_1} & e^{i\theta_2} & 1 + e^{i\theta_2} & 0 \end{pmatrix}.$$

Inserting $\theta = (0,0)$ and $\theta = (\pi, 0)$, we find

$$\sigma(\Delta^{(0,0)}) = \left\{0, \frac{6}{5}, \frac{8}{5}\right\} \quad \text{and} \quad \sigma(\Delta^{(\pi,0)}) = \{1 - \sqrt{5}^{-1}, 1 + \sqrt{5}^{-1}\}.$$

Again, these sets are disjoint whence Theorem 2.3 and Corollary 2.4 imply

Proposition 4.3. *The $(3^2.4.3.4)$-tiling has no $\ell^2(\mathcal{V})$-eigenfunctions.*

A fundamental domain consists of the six vertices $\{a, b, c, d, e, f\}$ around a hexagon, cf. Figure 13. It leads to the matrix

$$\Delta^\theta = \mathrm{Id} - \frac{1}{4}\begin{pmatrix} 0 & 1 & e^{-i(\theta_2-\theta_1)} & 0 & e^{i\theta_1} & 1 \\ 1 & 0 & 1 & e^{i\theta_1} & 0 & e^{i\theta_2} \\ e^{i(\theta_2-\theta_1)} & 1 & 0 & 1 & e^{i\theta_2} & 0 \\ 0 & e^{-i\theta_1} & 1 & 0 & 1 & e^{i(\theta_2-\theta_1)} \\ e^{-i\theta_1} & 0 & e^{-i\theta_2} & 1 & 0 & 1 \\ 1 & e^{-i\theta_2} & 0 & e^{-i(\theta_2-\theta_1)} & 1 & 0 \end{pmatrix}.$$
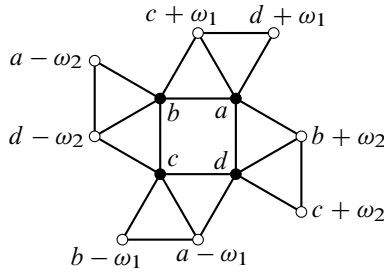
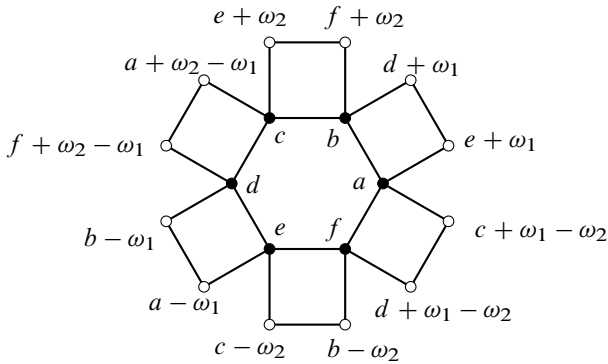Figure 12. Fundamental domain of the $(3^2.4.3.4)$ tiling.

Figure 13. Fundamental domain of the $(3.4.6.4)$ tiling.

4.4. IDS of the 3.4.6.4 tiling. We compare the spectra of Δ^θ at $\theta = (0, 0)$ and $\theta = (\pi, \pi/2)$:

$$\sigma(\Delta^{(0,0)}) = \left\{0, 1, \frac{3}{2}\right\}$$

and

$$\sigma(\Delta^{(\pi,\pi/2)}) = \left\{\lambda \in \mathbb{C}: \lambda^6 - 6\lambda^5 + \frac{57}{4}\lambda^4 - 17\lambda^3 + \frac{85}{8}\lambda^2 - \frac{13}{4}\lambda + \frac{95}{256} = 0\right\}.$$

It is straightforward to verify that these sets are disjoint. By Theorem 2.3 and Corollary 2.4, we find

Proposition 4.4. *The* (3.4.6.4) *tiling has no* $\ell^2(\mathcal{V})$-*eigenfunctions.*
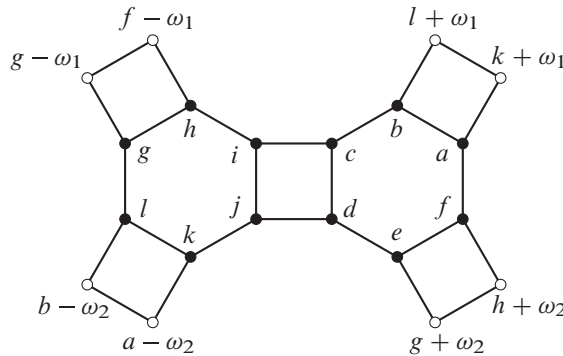

Figure 14. Fundamental domain of the (4.6.12) tiling.

4.5. IDS of the (4.6.12) tiling. A fundamental domain consists of the 12 vertices constituting two neighboring hexagons. This leads to

$$\Delta^\theta = \mathrm{Id} - \frac{1}{3}\begin{pmatrix} A & B \\ B^T & A \end{pmatrix},$$

where

$$A = \begin{pmatrix} 0 & 1 & 0 & 0 & 0 & 1 \\ 1 & 0 & 1 & 0 & 0 & 0 \\ 0 & 1 & 0 & 1 & 0 & 0 \\ 0 & 0 & 1 & 0 & 1 & 0 \\ 0 & 0 & 0 & 1 & 0 & 1 \\ 1 & 0 & 0 & 0 & 1 & 0 \end{pmatrix} \quad \text{and} \quad B = \begin{pmatrix} 0 & 0 & 0 & 0 & e^{\theta_1} & 0 \\ 0 & 0 & 0 & 0 & 0 & e^{\theta_1} \\ 0 & 0 & 1 & 0 & 0 & 0 \\ 0 & 0 & 0 & 1 & 0 & 0 \\ e^{\theta_2} & 0 & 0 & 0 & 0 & 0 \\ 0 & e^{\theta_2} & 0 & 0 & 0 & 0 \end{pmatrix}.$$

It suffices to study the spectrum of the adjacency matrix

$$M^\theta := \begin{pmatrix} A & B \\ B^T & A \end{pmatrix}$$

since the spectrum of M^θ differs from the spectrum of Δ^θ only by an invertible linear affine transformation. Thus, we need to check that there are θ, θ' such that $\sigma(M^\theta) \cap \sigma(M^{\theta'}) = \emptyset$. Plugging in the values $(0,0)$ and $(\pi, \pi/2)$ for θ, we find

$$\sigma(M^{(0,0)}) = \{\pm 1, \pm\sqrt{3}, \pm 3\}$$

and

$$\sigma(M^{(\pi,\pi/2)}) = \{\lambda \in \mathbb{C} \colon \lambda^{12} - 18\lambda^{10} + 111\lambda^8 - 268\lambda^6 + 207\lambda^4 - 50\lambda^2 + 1 = 0\}$$

and again it is straightforward to verify that these sets are disjoint whence also $\sigma(\Delta^{(0,0)}) \cap \sigma(\Delta^{(\pi,\pi/2)}) = \emptyset$. Theorem 2.3 and Corollary 2.4 imply

Proposition 4.5. *The (4.6.12)-tiling has no $\ell^2(\mathcal{V})$-eigenfunctions.*

4.6. IDS of the ($3^4.6$) tiling. A fundamental domain consists of the six vertices $\{a, b, c, d, e, f\}$ corresponding to a hexagon, cf. Figure 15. This leads to the matrix

$$\Delta^\theta = \mathrm{Id} - \frac{1}{5} \begin{pmatrix} 0 & 1 & e^{i\theta_2} & e^{i\theta_2} & e^{i\theta_1} & 1 \\ 1 & 0 & 1 & e^{i\theta_1} & e^{i\theta_1} & e^{-i(\theta_2-\theta_1)} \\ e^{-i\theta_2} & 1 & 0 & 1 & e^{-i(\theta_2-\theta_1)} & e^{-i(\theta_2-\theta_1)} \\ e^{-i\theta_2} & e^{-i\theta_1} & 1 & 0 & 1 & e^{-i\theta_2} \\ e^{-i\theta_1} & e^{-i\theta_1} & e^{i(\theta_2-\theta_1)} & 1 & 0 & 1 \\ 1 & e^{i(\theta_2-\theta_1)} & e^{i(\theta_2-\theta_1)} & e^{i\theta_2} & 1 & 0 \end{pmatrix}.$$
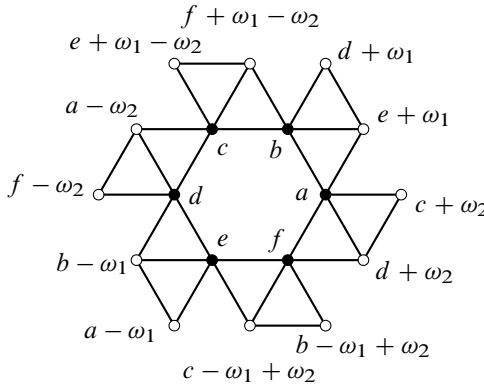

Figure 15. Fundamental domain of the ($3^4.6$) tiling.

We choose the particular values $\theta = (0,0)$ and $\theta = (\pi, \pi/2)$ and find

$$\sigma(\Delta^{(0,0)}) = \left\{0, \frac{6}{5}\right\}$$

and

$$\sigma(\Delta^{(\pi,\pi/2)}) = \Big\{\lambda \in \mathbb{C} \colon \lambda^6 - 6\lambda^5 + \frac{72}{5}\lambda^4 - \frac{2192}{125}\lambda^3$$
$$+ \frac{7056}{625}\lambda^2 - \frac{11192}{3125}\lambda + \frac{6656}{15625} = 0\Big\}.$$

It is straightforward to verify that these sets are disjoint and by Theorem 2.3 and Corollary 2.4 we find

Proposition 4.6. *The* $(3^4.6)$*-tiling has no* $\ell^2(\mathcal{V})$*-eigenfunctions.*

References

[1] L. Basnarkov and V. Urumov, Diffusion on Archimdean lattices. *Phys. Rev. E* **73** (2006), no. 4, article id. 046116, 5 pp.

[2] G. Berkolaiko and A. Comech, Symmetry and Dirac points in graphene spectrum. *J. Spectr. Theory* **8** (2018), no. 3, 1099–1147. MR 3831157 Zbl 1411.35092

[3] T. Bilitewski and R. Moessner, Disordered flat bands on the kagome lattice. *Phys. Rev. B* **98** (2018), no. 23, article id. 235109, 6 pp.

[4] P. Delplace and G. Montambaux, WKB analysis of edge states in graphene in a strong magnetic field. *Phys. Rev. B* **82** (2010), no. 20, article id. 205412, 21 pp.

[5] J. V. Field, Kepler's star polyhedra. *Vistas Astronom.* **23** (1979), no. 2, 109–141. MR 0546797

[6] F. C. Frank and J. S. Kasper, Complex alloy structures regarded as sphere packings. I. Definitions and basic principles. *Acta. Cryst.* **11** (1958), 184–190.

[7] F. C. Frank and J. S. Kasper, Complex alloy structures regarded as sphere packings. II. Analysis and classification of representative structures. *Acta. Cryst.* **12** (1959), 483–499.

[8] B. Grünbaum and G. C. Shephard, *Tilings and patterns.* An introduction. A Series of Books in the Mathematical Sciences. W. H. Freeman and Company, New York, 1989. MR 0992195 Zbl 0746.52001

[9] A. Harrison, First catch your hare: the design and synthesis of frustrated magnets. *J. Phys.*: *Condens. Matter* **16** (2004), S553–S572.

[10] B. Helffer, P. Kerdelhué, and J. Royo-Letelier, Chambers's formula for the graphene and the Hou model with kagome periodicity and applications. *Ann. Henri Poincaré* **17** (2016), no. 4, 795–818. MR 3472624 Zbl 1341.82125

[11] J. M. Hou, Light-induced Hofstadter's butterfly spectrum of ultracold atoms on the two-dimensional kagome lattice. *Chin. Phys. Lett.* **26** (2009), article id. 123701.

[12] J. L. Jacobsen, High-precision percolation thresholds and Potts-model critical manifolds from graph polynomials. *J. Phys. A* **47** (2014), no. 13, article id. 135001, 78 pp. MR3181081

[13] M. Keller, Curvature, geometry and spectral properties of planar graphs. *Discrete Comput. Geom.* **46** (2011), no. 3, 500–525. MR 2826967 Zbl 1228.05129

[14] J. Kepler, *Harmonices mundi.* Johann Plack, 1619.

[15] P. Kerdelhué and J. Royo-Letelier, On the low lying spectrum of the magnetic Schrödinger operator with kagome periodicity. *Rev. Math. Phys.* **26** (2014), no. 10, article id. 1450020, 46 pp. MR 3296397 Zbl 1309.35097

[16] H. Kesten, The critical probability of bond percolation on the square lattice equals $\frac{1}{2}$. *Comm. Math. Phys.* **74** (1980), no. 1, 41–59. MR 0575895 Zbl 0441.60010

[17] S. Klassert, D. Lenz, N. Peyerimhoff, and P. Stollmann, Elliptic operators on planar graphs: unique continuation for eigenfunctions and nonpositive curvature. *Proc. Amer. Math. Soc.* **134** (2006), no. 5, 1549–1559. MR 2199204 Zbl 1094.05016

[18] S. G. Krantz and H. R. Parks, *A primer of real analytic functions.* Basler Lehrbücher, 4. Birkhäuser Verlag, Basel, 1992. MR 1182792 Zbl 0767.26001

[19] P. A. Kuchment, On the Floquet theory of periodic difference equations. In C. A. Berenstein and D. C. Struppa (eds.), *Geometrical and algebraical aspects in several complex variables.* Papers from the conference held in Cetraro, June 1989. Seminars and Conferences, 8. Editoria Elettronica, Rende, 1991, 201–209. MR 1222215 Zbl 0979.39011

[20] P. A. Kuchment, An overview of periodic elliptic operators. *Bull. Amer. Math. Soc.* (*N.S.*) **53** (2016), no. 3, 343–414. MR 3501794 Zbl 1346.35170

[21] P. Kuchment and O. Post, On the spectra of carbon nano-structures. *Comm. Math. Phys.* **275** (2007), no. 3, 805–826. MR 2336365 Zbl 1145.81032

[22] D. Lenz, N. Peyerimhoff, O. Post, and I. Veselić, Continuity of the integrated density of states on random length metric graphs. *Math. Phys. Anal. Geom.* **12** (2009), no. 3, 219–254. MR 2525593 Zbl 1179.35333

[23] D. Lenz, N. Peyerimhoff, and I. Veselić, Groupoids, von Neumann algebras and the integrated density of states. *Math. Phys. Anal. Geom.* **10** (2007), no. 1, 1–41. Zbl 1181.46046

[24] D. Lenz and I. Veselić, Hamiltonians on discrete structures: jumps of the integrated density of states and uniform convergence. *Math. Z.* **263** (2009), no. 4, 813–835. MR 2551600 Zbl 1183.82082

[25] V. Mathai and S. Yates, Approximating spectral invariants of Harper operators on graphs. *J. Funct. Anal.* **188** (2002), no. 1, 111–136. MR 1878633 Zbl 1041.47013

[26] M. Mekata, Kagome: The story of the basketweave lattice. *Phys. Today* **56** (2003), no. 2, 12–13.

[27] R. Parviainen, Estimation of bond percolation thresholds on the Archimedean lattices. *J. Phys. A* **40** (2007), no. 31, 9253–9258. MR 2345290 Zbl 1121.60101

[28] N. Peyerimhoff, M. Täufer, and I. Veselić, Unique continuation principles and their absence for Schrödinger eigenfunctions on combinatorial and quantum graphs and in continuum space. *Nanosystems*: *Physics, Chemistry, Mathematics* **8** (2017), no. 2, 216–230.

[29] P. N. Suding and Robert M. Ziff, Site percolation thresholds for Archimedean lattices. *Phys. Rev. E* **60** (1999), no 1, 275–283.

[30] M. F. Sykes and J. W. Essam, Exact critical percolation probabilities for site and bond problems in two dimensions. *J. Mathematical Phys.* **5** (1964), 1117–1127. MR 0164680

[31] K. Ueda, T. Dotera, and T. Gemma, Photonic band structure calculations of two-dimensional Archimedean tiling patterns. *Phys. Rev. B* **75** (2007), no. 19, article id. 195122, 11 pp.

[32] P. R. Wallace, The band theory of graphite. *Phys. Rev.* (2) **71** (1947), 622–634. Zbl 0033.14304

[33] X. Zhao, J. C. Wu, Z. Y. Zhao, Z. Z. He, J. D. Song, J. Y. Zhao, X. G. Liu, X. F. Sun, and X. G. Li, Heat switch effect in an antiferromagnetic insulator $Co_3V_2O_8$. *Appl. Phys. Lett.* **108** (2016), article id. 242405.

Norbert Peyerimhoff, Durham University, Science Laboratories, South Road, Durham, DH1 3LE, United Kingdom

e-mail: norbert.peyerimhoff@durham.ac.uk

Matthias Täufer, FernUniversität in Hagen, Fakultät für Mathematik und Informatik, 58084 Hagen, Germany

e-mail: matthias.taeufer@fernuni-hagen.de